

Resolving heterogeneity in CO₂ uptake potential in the Greenland coastal ocean

Henry C. Henson^{1,2,*}, Mikael Sejr^{1,2}, Lorenz Meire^{3,4}, Lise Lotte Sørensen^{2,5}, Mie HS Winding³, Johnna M. Holding^{1,2}

¹Department of Ecoscience, Aarhus University, Denmark

²Arctic Research Centre, Aarhus University, Denmark

³Greenland Climate Research Centre, Greenland Institute of Natural Resources, Nuuk, Greenland

⁴Department of Estuarine and Delta Systems, Royal Netherlands Institute for Sea Research, Yerseke, the Netherlands

⁵Department of Environmental Science, Aarhus University, Denmark

Corresponding Author: Henry C. Henson (hch@ecos.au.dk)

Key Points:

- The Greenland coastal ocean takes up large quantities of carbon dioxide yet displays considerable spatial heterogeneity.
- Biology and freshwater runoff control pCO₂ levels to varying degrees in different regions.
- Estimation of the true flux magnitude is beset by large uncertainties, particularly in polar coastal regions.

Abstract

The oceans play a pivotal role in mitigating climate change by sequestering approximately 25% of annually emitted anthropogenic carbon dioxide (CO₂). High-latitude oceans, especially the Arctic continental shelves, emerge as crucial CO₂ sinks due to their cold, low saline, and highly productive ecosystems. However, these heterogeneous regions remain inadequately understood, hindering accurate assessments of their carbon dynamics. This study investigates variation in pCO₂ levels during peak ice sheet melt, in the Greenland coastal ocean and estimates rates of air-sea exchange across 6° of latitude. The East and West coast of Greenland displayed distinct regions with unique controlling factors. Though, both coasts represent CO₂ sinks in summer. Geographical variation in pCO₂ and air-sea exchange was linked intricately to freshwater export from the Greenland ice sheet and levels of primary production in these ecosystems. CO₂ uptake ranged from 0.17 to -38 mmol m⁻² day⁻¹. However, we found that flux estimation faces substantial uncertainties (up to 770%) due to wind product averaging and gas exchange formula selection. Despite these considerations, we report a first order estimate that Greenland coastal ocean takes up -9.5 ± 9.0 Tg C year⁻¹, corresponding to nearly 4% of global coastal CO₂ uptake. Obtaining a reliable assessment of air-sea CO₂ exchange necessitates data collection across seasons, and, even more so, refinement of the gas transfer velocity estimations in the Arctic coastal zone.

Plain Language Summary

The oceans help to limit climate change by absorbing large amounts (1/4) of carbon dioxide (CO₂) that humans emit to the atmosphere. The majority of this CO₂ enters the oceans near the poles due to the special conditions that occur in these regions: namely that there is cold, less salty water, with high quantities of photosynthetic algae in the surface ocean. However, scientists do not completely understand the regional variability of oceanic CO₂ uptake, which limits our ability to accurately predict future climate scenarios. This study measured the partial pressure of CO₂ in the ocean along East and West Greenland to calculate rates of air-sea transfer. CO₂ uptake ranged from 0.17 to -38 mmol m⁻² day⁻¹ and the controlling factors behind this flux of carbon were wind speed, amount of glacial runoff, and the balance between biologic producers/consumers. The Greenland coastal ocean may represent nearly 4% of global coastal ocean CO₂ uptake, indicating the need to better understand carbon sequestration variability in this region.

Introduction

The world's oceans serve as a critical buffer against the escalating impacts of anthropogenic carbon dioxide (CO₂) emissions, absorbing approximately 25% of these emissions annually (Ciais et al., 2013; Sabine, 2004; Takahashi et al., 2009). Oceans at high latitudes uptake more of this CO₂ due to a combination of low temperatures and high productivity (Bates and Mathis, 2009; Takahashi et al., 2009). Although 25% of continental shelves (depth < 200 m) are located in the Arctic, we still have a limited understanding of the carbon dynamics in these high-latitude coastal systems due to the lack of field observations compared to low-latitude coastal environments (Bates and Mathis, 2009).

The driving force behind CO₂ exchange across the sea surface is the difference in partial pressure of CO₂ ($\Delta p\text{CO}_2$) between seawater and the overlying air. However, the fluctuation of oceanic pCO₂ is more spatially and temporally variable compared to atmospheric pCO₂, making oceanic pCO₂ the thermodynamic driver of air-sea carbon uptake. Arctic coastal waters, are generally considered as a sink for CO₂ due to their undersaturated pCO₂ conditions throughout the year (Ahmed et al., 2020; Dai et al., 2022; Laruelle et al., 2014, 2018). Some distinct regions, such as the Siberian shelf seas, exhibit CO₂ effluxes due to decomposition of abundant terrestrial organic matter (Anderson et al., 2009). However, other coastal regions, where net-autotrophy dominates, remain large atmospheric carbon sinks (e.g. Meire et al., 2015). Still, the magnitude and relative driving processes in shelf seas remain poorly quantified. The coastal ocean is unique, in that it is influenced both by the local environment on land, as well as larger oceanic and atmospheric circulation. These coastal systems play a pivotal role in ocean-atmosphere dynamics due to their large exchanges of matter and energy (e.g., heat, CO₂, water) at their interfaces, yet have often been overlooked in air-sea exchange surveys due to their spatial and temporal complexity (Chen and Borges, 2009; Miller et al., 2019).

Understanding the intricate dynamics of CO₂ exchange in Greenland's coastal ocean is imperative given the heterogeneous nature of its coastline. A few previous studies have estimated air-sea exchange in Greenland fjords (Meire et al., 2015; Rysgaard et al., 2012; Sejr et al., 2011). However, these studies estimate fluxes from only two fjord systems, and have previously been used to upscale for the entire Greenland coastal ocean (eg. Laruelle et al., 2013). Knowing that the coasts of Greenland are a heterogeneous landscape, it is crucial we gain a better understanding of the spatial variation in pCO₂ levels and carbon fluxes in this region to obtain reliable assessments of the CO₂ uptake by the Greenlandic coastal area. Additionally, a large-scale perspective on the drivers of surface pCO₂ levels is necessary to gauge if the combined effects of climate change will result in a positive or negative feedback on coastal carbon uptake. We expect that a glacial meltwater and biological activity will drive heterogeneity in pCO₂ levels because carbon dynamics are controlled by a combination of abiotic and biotic factors (Henson et al. 2023). However, the relative contribution of these drivers as well as the magnitude of this heterogeneity have not been examined for CO₂ fluxes in this region. This study aims to fill in this gap in knowledge by exploring CO₂ fluxes in Greenlandic fjords and shelf waters spanning 6° of latitude. Given the region's sensitivity to climate change and its substantial CO₂ uptake relative to other marine areas, a realistic assessment of exchange rates is imperative. By delving into the drivers influencing air-sea CO₂ exchange in these coastal waters, we strive to contribute valuable insights toward a more comprehensive understanding of the role played by high-latitude coastal systems in the global carbon cycle.

Methods

Sampling

Two research cruises were conducted along the coasts of Greenland where oceanic partial pressure of CO₂ (pCO₂) and other environmental parameters were measured. The first cruise, along the western coast of Greenland (69–75°N) was conducted during 12–30 August 2016. Meanwhile, the second cruise along the eastern coast of Greenland (68–74°N) was conducted between July 30 and August 24, 2018 (Fig. 1). Additional stations in Young Sound, East Greenland were sampled in 2018 as part of the Greenland Ecosystem Monitoring program (Christensen et al., 2017; Sejr et al., 2011). Seawater pCO₂ profiles were measured using a Contros Hydro-C CO₂ sensor (Meire et al., 2023). The Hydro-C sensor was equilibrated for 5–10 min until a stable reading was acquired at 8 depths between 1–60m (1m, 5m, 10, 20m, 30m, 40m, 50m, 60m). The relative standard deviation of the Contros pCO₂ measurement has been estimated to be 1% (Fietzek et al., 2014). While some in the research community argue that membrane-based sensors are less precise, we posit that measurement from underway systems in highly stratified waters poses as much or more error when calculating air-sea exchange (Macovei et al., 2021; Miller et al., 2019). Therefore, membrane-based sensors at 1m allowed a robust examination of surface layer pCO₂ values in coastal Greenland waters. At each station, depth profiles of temperature and salinity, were obtained using CTD instruments (SBE19 + V2 and SBE25 on West and East coast cruises respectively), equipped with additional sensors for chlorophyll-a fluorescence, photosynthetically available radiation (PAR), and dissolved oxygen (Bendtsen et al., 2017; Carlson et al., 2020; Holding et al., 2021). Dissolved oxygen sensors were calibrated using Winkler titrations using water samples collected in Niskin bottles. During the western cruise, 56 CTD casts were conducted with 53 stations measured for pCO₂. Meanwhile the eastern cruise conducted 89 CTD casts, with pCO₂ profiles measured at 63 stations. Through visual examination of satellite imagery, stations in the very inner fjord arms, were categorized based on the prevalent glacial output (marine- or land-terminating, “MTG” and “LTG” respectively). When a station was located in the larger, more outer fjord system with influence from many different sources of freshwater it was categorized as just “fjord,” and when a station was located outside the fjord mouth, they were assigned as “shelf” stations (Supplemental Fig. 1).

Calculation of air-sea exchange

The net air-sea exchange of CO₂ was calculated using the diffusive boundary model (Sejr et al., 2011):

$$(1) F = k_{660}s(\Delta pCO_2)$$

where F is the flux of CO₂, k_{660} is the gas transfer velocity normalized to 20°C and a salinity of 35 PSU, s is the solubility of CO₂ in seawater, and ΔpCO_2 is the difference between atmospheric and surface water pCO₂ values (at 1m depth). Atmospheric pCO₂ levels were obtained from the SeaFlux data product (Fay et al., 2021; Gregor, 2023) in August of 2016 and 2018 at each measurement location. The solubility of CO₂, s , was calculated according to Weiss (1974) using surface water temperature and salinity from CTD casts. Gas transfer velocities (k_{660}) were normalized according to: $k_{660} = k(660/Sc)^{-0.5}$ where the Schmidt number (Sc), was calculated following Wanninkhof (1992). The gas transfer velocity, k , is a product of turbulence and is often estimated based on empirically derived relationships with wind speed in oceanic environments. A variety of formulas have been proposed based on different datasets from varying regions. We chose the formulation by Nightingale et al. (2000) as it was derived for coastal environments and has been used in previous assessments of CO₂ fluxes around the Greenland coast (Meire et al., 2015; Rysgaard et al., 2012; Sejr et al., 2011)

$$(2) k = 0.333U_{10} + 0.222U_{10}^2,$$

where U_{10} is wind speeds (m s^{-1}) at 10 m above sea surface. Wind speeds were obtained from the Copernicus Arctic Regional Reanalysis (Copernicus Climate Change Service, 2021) and averaged over the months of August 2016 and 2018.

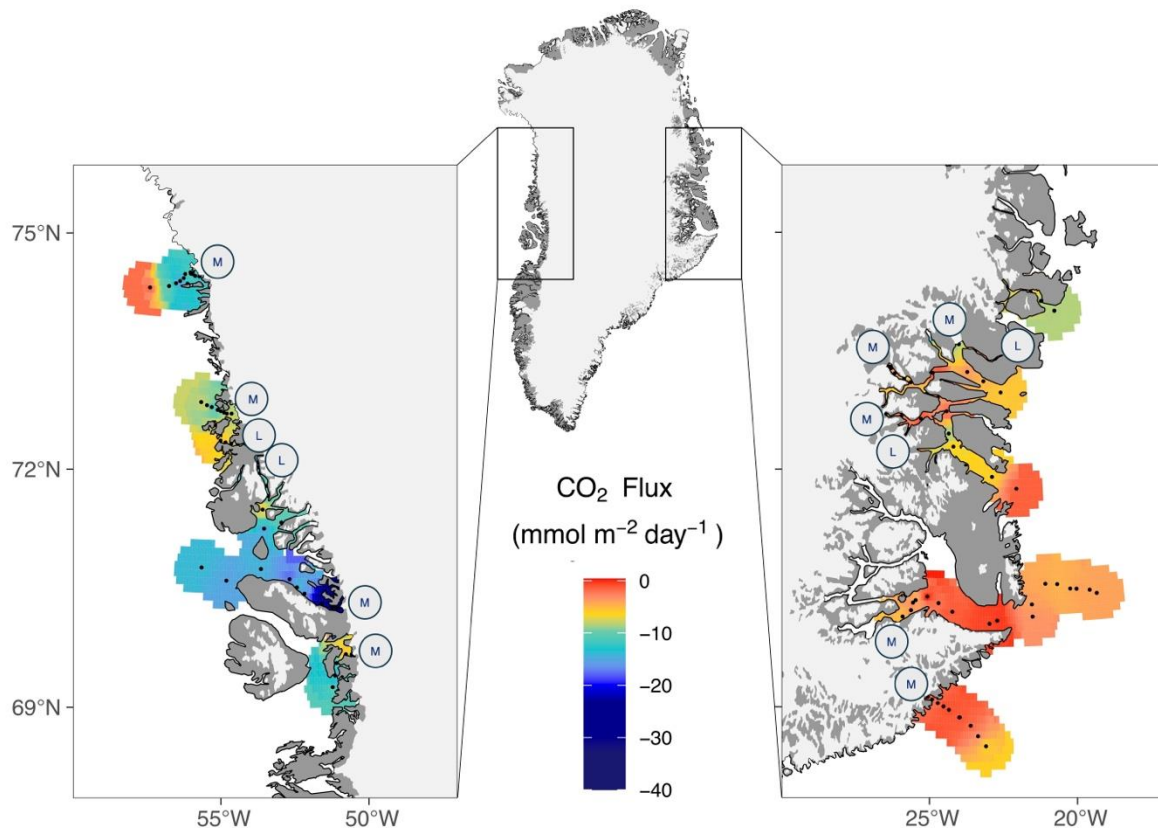


Figure 1: Map of air-sea exchange of CO_2 in Greenland coastal waters. Station locations are pictured as black points. Data was interpolated using an inverse distance weighted matrix limited to a maximum distance of 39 km. Marine- and Land-terminating glaciers are labeled with M and L respectively.

Statistical Modelling

In order to examine the impact of environmental parameters on surface layer pCO_2 levels, statistical models were applied to our data. First, general linear models were fit to identify relationships between predictors and pCO_2 in the upper 20 m. Model parameters were chosen based on the reduction of Akaike's information criterion (AIC) and verified using likelihood ratio tests. Multicollinearity was evaluated and limited using calculated variance inflation factors.

Spatial autocorrelation is often a feature of large-scale biodiversity and ecological data (Kreft and Jetz, 2007), making it necessary to check for a spatial structure of our data. Plotting residuals and conducting a Moran's I test confirmed there is spatial structure to our data (Moran I = 0.36, p -value < 5×10^{-5}). Spatial autocorrelation can inflate type 1 errors and potentially influence parameter estimation (Kreft and Jetz, 2007), making it necessary to correct for spatial autocorrelation. Generalized least squares models (GLS) with spatial structures as well as spatial autoregressive models were fit to model pCO_2 . Final spatial linear model (SLM) selection was based on the reduction of spatial autocorrelation in the residuals and the minimization of AIC values. A spatial GLS model with a rational quadratics spatial correlation structure performed the best for modeling response data. A likelihood ratio test confirmed that adding a rational quadratic spatial correlation

structure was significantly better than the base model ($p\text{-value} < 5e-4$). In order to construct this model, a spatial weights matrix was fit using $k = 1$ nearest neighbors. The correlogram of the fitted model illustrated that the problem with spatial autocorrelation had been successfully accounted for.

Results

Heterogeneity and drivers of $p\text{CO}_2$

Comparison between the east and west coasts of Greenland revealed differences extending beyond surface waters. Depth profiles of $p\text{CO}_2$ depicted distinct signals in both regions. Western Greenland exhibited more variable $p\text{CO}_2$ values with depth, displaying high undersaturation (94-364 μatm) in surface waters and CO_2 accumulation (291-522 μatm) already at a depth of 50 meters (Fig. 2, Supplemental Fig. 2). Conversely, the eastern coast displayed more uniform $p\text{CO}_2$ levels across the mixed layer, with values slightly below atmospheric levels (221-399 μatm at 1 m and 330-414 at 50 m; Fig. 2).

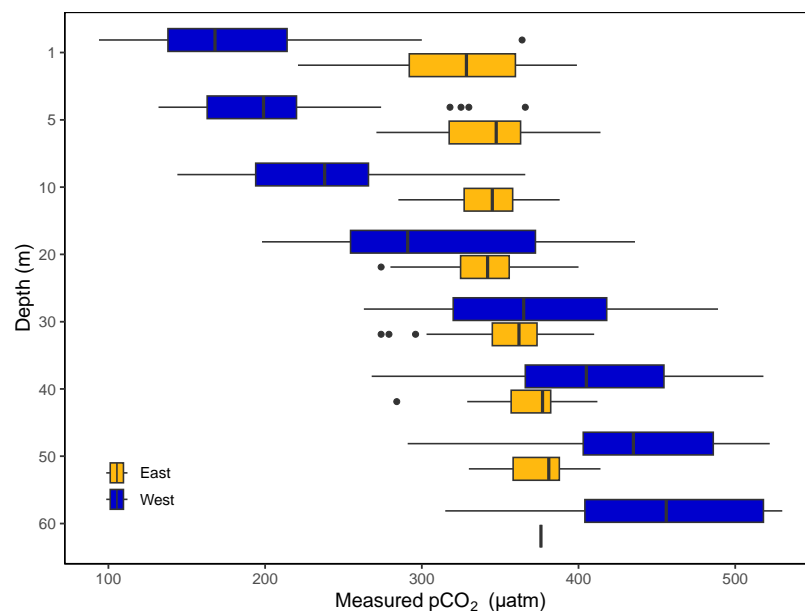


Figure 2. Boxplots of $p\text{CO}_2$ profiles on the East and West coast of Greenland.

The concentrations of $p\text{CO}_2$ in the water column are influenced by a combination of biological and physical/chemical factors. The main drivers affecting $p\text{CO}_2$ are depicted in Figure 3. Apparent Oxygen Utilization (AOU), also known as the deviation from O_2 saturation, serves as a valuable indicator of biological activity (e.g. Sejr et al., 2014). Positive AOU values imply bacterial O_2 consumption, while negative values signify photosynthetic O_2 production. Along the western coast of Greenland, AOU showed a strong correlation with measured $p\text{CO}_2$. Primary producers' biological incorporation of carbon decreased $p\text{CO}_2$ levels in the surface layer (Fig. 3a). Conversely, deeper waters exhibited net respiration, where O_2 consumption and CO_2 production took place concurrently. Along the Eastern coast of Greenland, lower levels of net production and net respiration were observed (Fig. 3b), leading to a decoupling between AOU and measured $p\text{CO}_2$. This region, known for its lower productivity (Henson et al., 2023), exhibited less variation in $p\text{CO}_2$ levels.

Figures 3c and 3d highlight the primary physical and chemical drivers of $p\text{CO}_2$ in this region: freshwater influx. Glacial meltwater input has been documented to reduce seawater $p\text{CO}_2$ through both thermodynamic effects and dilution (Meire et al., 2015). The relationship between freshwater input and $p\text{CO}_2$ is apparent in both eastern and western Greenland, where the lowest $p\text{CO}_2$ levels

correspond with lower salinities. However, a stronger relationship was observed, in eastern Greenland where low levels of biological production, and fewer high salinity values make this relationship more apparent.

These relationships were confirmed using statistical models. This study applied a generalized least squares (GLS) model incorporating a rational quadratic spatial correlation structure to examine the dynamics of pCO₂ in relation to environmental predictors. Fit model parameters are shown in Table 1. Two interactions helped to improve model fit: the interaction between coast & AOU as well as the interaction between coast & temperature, illustrating the different effects of biology in each coast. Both biological and physical factors emerged as robust predictors for surface layer pCO₂ levels. The spatial model illustrates that in western Greenland, fluctuations in pCO₂ were primarily driven by AOU (biological processes). Conversely, in eastern Greenland, salinity and temperature exerted the most substantial influence on pCO₂ levels. This spatial linear model duly accounted for the spatial autocorrelation of measured pCO₂ values. The estimated range (distance at which spatial correlation becomes negligible) is approximately 1.15 longitudinal degrees, and the nugget parameter (unaccounted variability) was 0.43.

Table 1. Fitted GLS model with rational quadratic spatial structure.

	Estimate	T statistic	p-value
Intercept	108.3	4.214	<0.0001
AOU	0.016	0.230	0.8180
Salinity	6.718	10.56	<0.0001
Temperature	12.66	8.719	<0.0001
Coast (west)	-53.96	-2.318	<0.0001
AOU:Coast (west)	0.770	7.068	<0.0001
Temperature:Coast (west)	-11.72	-6.140	<0.0001

Model performance underwent rigorous assessment via cross-validation, utilizing subsets of the dataset to train and validate the model (Table 2). Our spatial linear model (SLM) accurately predicted 83% of the variance in pCO₂ within the test dataset, indicating that a relatively simple model can accurately estimate coastal pCO₂ levels. This robust predictive capacity was further supported by the evaluation metrics: the root mean standard error (RMSE) and mean absolute error (MAE). These metrics indicated an average and absolute difference of 36.2 and 27.8 µatm, respectively, between the predicted and actual pCO₂ values. Therefore, knowledge of the spatial heterogeneity in temperature, salinity, and AOU (or magnitude of auto/heterotrophy) could be used to estimate or explain variability in surface water pCO₂ around coastal Greenland.

Table 2. GLS model cross validation

R-squared	RMSE	MAE
0.836	36.2 µatm	27.8 µatm

Spatial variability in pCO₂ could also be explained by circulation-driven glacial effects. The entry of glacial meltwater into fjord waters occurs at varying depths, contingent upon whether the fjord contains an outlet glacier that is marine- or land-terminating (MTG and LTG, respectively). This inflow dramatically influences the circulation within fjords (Mortensen et al., 2014). Surface runoff from land-terminating glaciers resulted in a warmer, fresher surface layer (Henson et al., 2023). In these turbid waters on the western coast of Greenland, oxygen production, indicative of primary production, was limited compared to near marine terminating glaciers (p-value < 5e-5) where

subglacial discharge drives upwelling of nutrient-rich bottom water. Meanwhile, AOU did not vary spatially on the east coast (Fig. 4a). Similar to AOU, pCO₂ values in western Greenland were elevated near LTGs compared to near MTGs, with even higher values in shelf waters (Fig. 4b). Eastern Greenland did not demonstrate a difference in pCO₂ values between stations near LTGs and MTGs (p-value = 0.997). However, the stations close to glacial output exhibited lower pCO₂ values than mid-fjord or shelf waters (Fig. 4b).

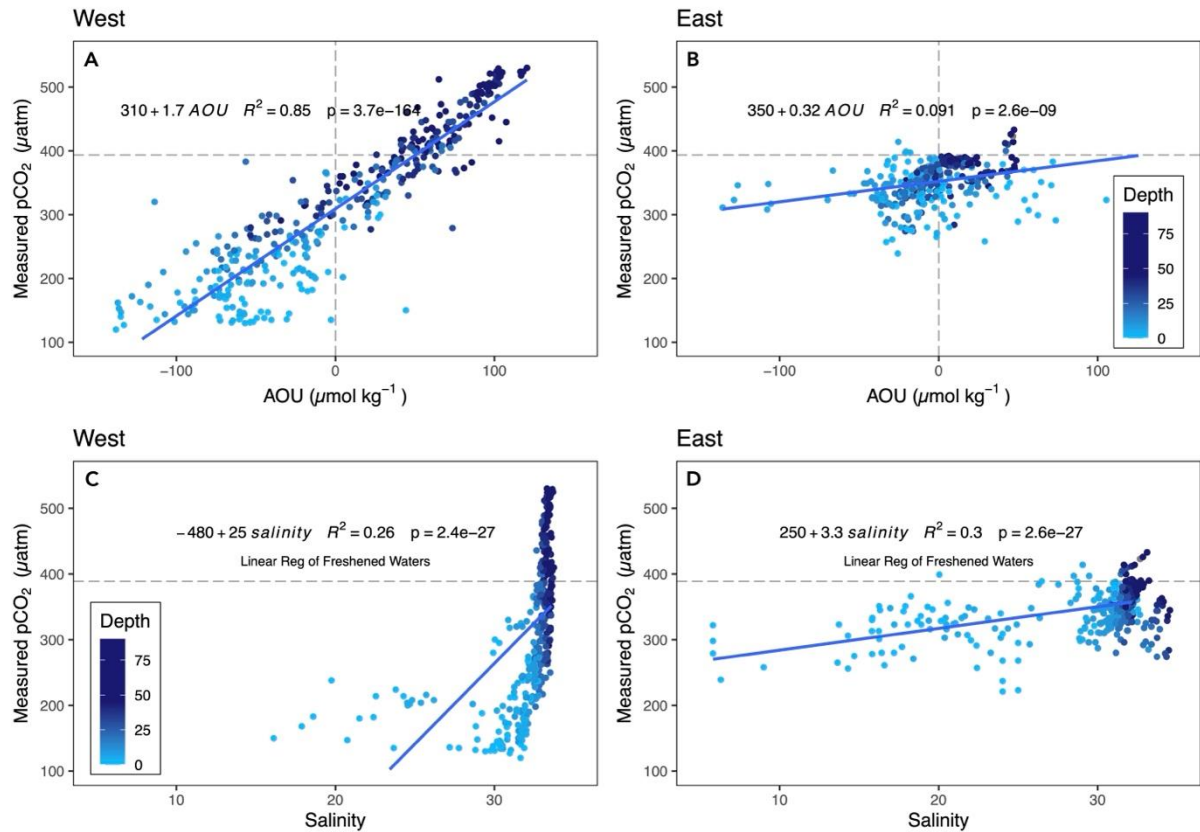


Figure 3. Relationships between apparent oxygen utilization (AOU) and pCO₂ (a, b) and salinity and pCO₂ (c, d) for East and West coasts. Linear regression fits use all data in a & b while c & d fit regression for all data below salinity of coastal seawater endmembers (Henson et al. 2023). Atmospheric pCO₂ concentrations and the equilibrium between net auto- and heterotrophy are depicted with horizontal and vertical gray dashed lines respectively.

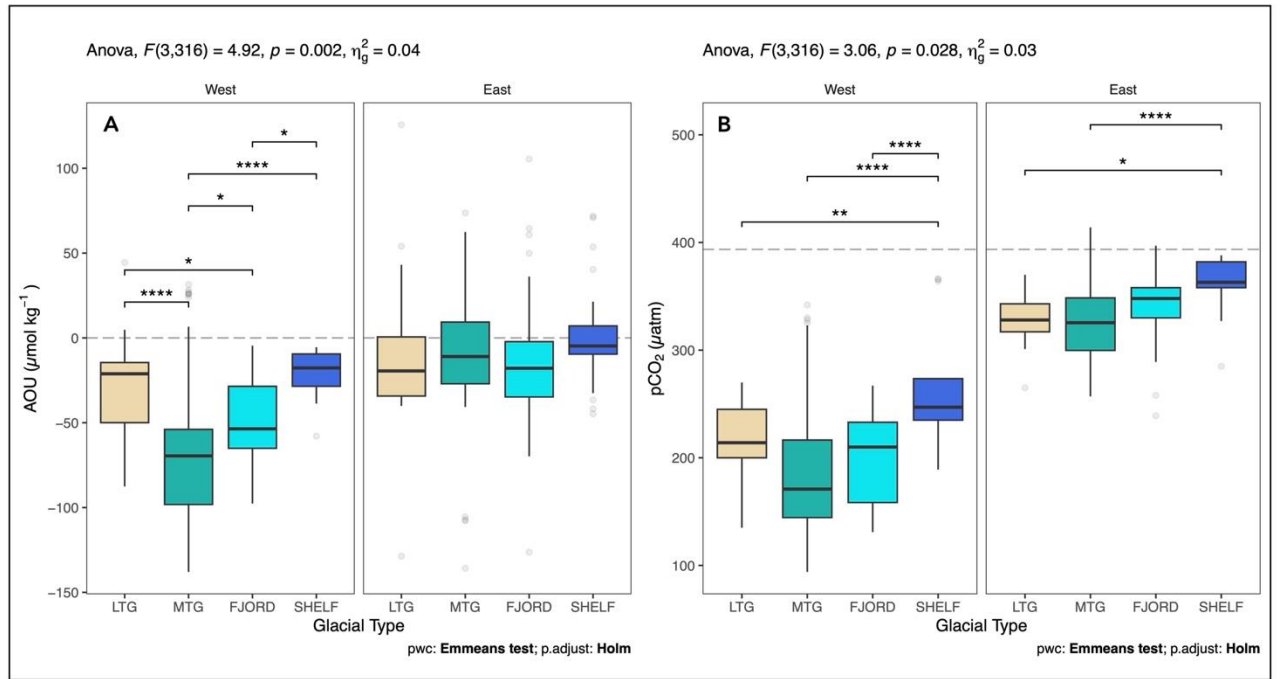


Figure 4. Boxplots and two-way ANOVA analysis of AOU with fjord location (a) and pCO₂ (b) with fjord location for surface layer samples (above 20 m depth). Significant interactions between coast and fjord location on AOU and on pCO₂ are described above each plot. All pairwise comparisons were analyzed between the different fjord location groups organized by coast. Statistical differences are depicted as brackets above boxplots with significance codes. Non-significant pairwise comparisons are not pictured. Equilibrium between net auto- and heterotrophy (a) as well as atmospheric pCO₂ concentrations (b) are depicted as gray dashed lines.

CO₂ Fluxes

The air-sea exchange of CO₂ is a product of wind speed driven turbulence and $\Delta p\text{CO}_2$. Understanding the interplay between these factors is crucial in understanding the dynamics of CO₂ fluxes in marine environments. In our investigation, we delve into the impact of wind speed on this exchange, examining fluxes calculated from both monthly and three-hour wind speed averages. The monthly wind speeds in August ranged between 1.7 to 6.5 m s⁻¹ across our stations within Greenland fjords while three-hour averages ranged from 0-16.6 m s⁻¹. Notably, we found a strong correlation ($R^2 = 0.77$; $P = 1.1\text{e-}36$) between these two flux calculations. However, the air-sea CO₂ flux derived from three-hour wind averages exceeded the estimates from monthly wind speeds by an average of 10%. Disparities in these calculations are attributed to the non-linear relationship between gas transfer velocity and wind speed (Eq. 2), leading to significant exchanges during periods of high wind speed events. As a result, if 1hr or 10 min average wind speeds were available, one could expect an even larger difference to monthly averages.

In August, both the East and West coasts of Greenland showed pCO₂ values in surface water below atmospheric levels, indicating this region acts as a CO₂ sink. However, considerable geographic variability existed in $\Delta p\text{CO}_2$ values, leading to varied flux magnitudes. Fluxes in West Greenland ranged from -37.52 to -1.80 mmol m⁻² day⁻¹ while those in East Greenland ranged from -13.24 to 0.17

mmol m⁻² day⁻¹, highlighting differences in sink capacity and controlling factors between regions. Despite regional variations, certain trends emerged. The highest CO₂ uptake was observed near the Greenland ice sheet, whereas lower uptake, driven by smaller ΔpCO₂, was recorded in shelf waters (Fig. 1). These glacial fjords therefore shape a gradient between sources of freshening and the open ocean, displaying a transition from more negative to less negative fluxes.

Discussion

Greenland coastal pCO₂ is highly heterogeneous

Our observation of low surface water pCO₂ in coastal Greenland waters affirm the previous conclusions of Sejr et al. (2011, 2014), Meire et al. (2015, 2023), and Rysgaard et al. (2012) that these waters are large CO₂ sinks. We measured ΔpCO₂ values ranging from -295 to 5 μatm with an average of -127 μatm. Only a single measurement was above atmospheric levels and was located in Kangertittivaq. These measurements, while displaying wide variation, represent similar values to summer measurements in other regions of coastal Greenland. Sejr et al. (2011) observed averages between -77 to -134 μatm in Young Sound, Rysgaard et al. (2012) observed ΔpCO₂ values between -20 and -330 μatm in offshore areas of Southern Greenland and Meire et al. (2015) measured between -115 and -323 μatm within the Nuup Kangerlua fjord system. These seem analogous to the variability and levels of ΔpCO₂ that we observed on the east and west coast. Additionally, when comparing to syntheses of global shelf seas, our measured ranges of ΔpCO₂ fall within low-end of measurements at the same latitude (Dai et al., 2022).

Although pCO₂ values have been reported before, this is the first study to examine CO₂ uptake potential in more than one fjord system. We measured pCO₂ levels across 6° of latitude in both East and West Greenland and discovered quite different ecosystems comparing the two coasts. The observed spatial variability of pCO₂ emerges as a consequence of multifaceted oceanographic factors (Meire et al., 2015; Sejr et al., 2011). Therefore, understanding spatial flux variability requires an understanding of the environmental drivers of marine carbon dynamics.

Autotrophy/Heterotrophy balance dictates pCO₂ in West Greenland

Both biological and physical parameters were found to be significantly related to surface water pCO₂ within SLM models (Table 1). As a result, oxygen saturation in combination with salinity and temperature can be used to predict surface layer pCO₂ levels in coastal Greenland waters. This is because biological processes dictate levels of dissolved inorganic carbon (DIC) within the water column (Henson et al., 2023). The uptake of DIC by primary production reduces its concentration in seawater, while bacterial decomposition acts as a source of DIC. This direct consumption and production of DIC helps to explain the strong spatial link between pCO₂ levels and AOU in western Greenland fjords (Fig. 3a). Similarly, limited biological productivity in eastern Greenland resulted in less variability in pCO₂ profiles with depth (Fig. 2). Western Greenland is known to be more productive ecosystem compare to eastern Greenland (Henson et al., 2023; Vernet et al., 2021). Primary production in the photic zone consumes DIC at the expense of deeper waters. In areas exhibiting elevated photosynthesis, increased amounts of particulate organic matter sink below the photic zone and undergo remineralization (Arendt et al., 2010; Henson et al., 2023). Nevertheless, the specific impact of the biological pump compared to the advection of shelf water on pCO₂ levels remains uncertain.

Glacial meltwater lowers pCO₂ levels along the coasts of Greenland

Our other primary environmental driver of $p\text{CO}_2$ variability in these ecosystems is meltwater runoff from the Greenland ice sheet. Freshwater input to coastal waters has two main effects: it alters pelagic biological production by modifying water mass circulation within the fjords and induces direct physical and chemical changes.

Fjords influenced by land-terminating glaciers (LTGs) showcase distinctive characteristics marked by pronounced thermohaline stratification due to glacial river runoff (Henson et al., 2023). Heightened turbidity and stratification-driven nutrient limitation restrict primary production (Henson et al., 2023; Meire et al., 2017) and therefore CO_2 uptake in surface waters. Conversely, subglacial meltwater from marine-terminating glaciers (MTGs) generates buoyant plumes near glacier termini. These plumes entrain nutrient-rich water, stimulating phytoplankton blooms, and contribute to the reduction of surface DIC in fjords where MTGs are present (Chierici and Fransson, 2009; Henson et al., 2023; Meire et al., 2015, 2017; Rysgaard et al., 2012). However, these buoyant plumes may also entrain DIC-rich bottom water, elevating $p\text{CO}_2$ below the photic zone. Therefore, freshwater-driven circulation dynamics play a pivotal role in dictating the location and intensity of biological DIC consumption, thereby impacting the magnitude of air-sea exchange. Indeed, a recent study found that neighboring fjords with different glacial termini showed double the carbon uptake near MTGs compared to near LTGs (Meire et al., 2023). This relationship is evident in West Greenland, where the spatial distribution of AOU closely corresponds to the distribution of surface layer $p\text{CO}_2$ values (Fig. 4). However, this association seems absent in Eastern Greenland where no apparent difference in biological activity or $p\text{CO}_2$ levels near the termini of MTGs or LTGs are observed. This discrepancy might be attributed to the source history of water masses along the East Coast. Seawater entering fjords from the East Greenlandic current consists of cold, nutrient-poor water originating from the Arctic outflow (Henley et al., 2020). This combined with relatively lower glacial discharge (Velicogna et al., 2020) results in reduced upwelling of already nutrient-limited water and therefore restricted primary production along the East Coast, even near marine-terminating glaciers.

Freshwater input also has direct impacts on coastal carbon dynamics. A distinct relationship between $p\text{CO}_2$ and salinity was clearly visible (Figure 3c, 3d). Lowest observed $p\text{CO}_2$ values and therefore the strongest carbon sinks had low salinities and were located near the glacial termini (Figure 3c, 3d, 4b). Greenland's coastal waters are profoundly impacted by freshwater inputs. Within these fjords, August freshwater fractions were primarily of glacial origin while sea ice melt was limited (Henson et al., 2023). When compared to regions like Svalbard and Hudson Bay, Greenland stands out for its unique freshened waters characterized by lower salinity levels and ^{18}O isotopic signatures (Azetsu-Scott et al., 2010; Ericson et al., 2019; Fransson et al., 2015; Granskog et al., 2011; Henson et al., 2023). This freshwater has physical and chemical effects on the carbon dynamics of seawater. Glacial fjords, particularly affected by freshening, experience enhanced CO_2 undersaturation due to the non-linear influence of salinity on $p\text{CO}_2$ (Meire et al., 2015; Rysgaard et al., 2012). The combination of low temperatures, $p\text{CO}_2$ undersaturation, and the non-linear relationship with salinity amplifies the potential for CO_2 uptake in surface waters within fjords where freshening occurs.

As we anticipate increased melting in the future, one might expect a larger $\Delta p\text{CO}_2$ and air-sea exchange. However, while increased melting may augment carbon uptake through freshening-driven CO_2 drawdown, future climate change may in some circumstances have the reverse effect. As temperatures increase, surface water warming could limit gas dissolution and decrease $\Delta p\text{CO}_2$ between the ocean and the atmosphere. Additionally, the transition from MTGs to LTGs due to glacial retreat may lead to a reduction in primary production, limiting air-sea CO_2 exchange (Meire et al., 2023).

Air-sea exchange and sources of uncertainty

Flux magnitudes are a product of not only $\Delta p\text{CO}_2$ but also gas transfer velocity. This diffusion of gases is related to wind-driven turbulence at the air-sea interface. The interplay between wind speed and $\Delta p\text{CO}_2$ values plays a pivotal role in shaping these fluctuations (Ho et al., 2011). Spatial variability in summer fluxes around Greenland, therefore, are dictated not only by carbon dynamics but also wind regimes and fjord morphology. Notably, regions experiencing extreme CO_2 uptake, such as Uummannaq Fjord, exhibit a convergence of both larger $\Delta p\text{CO}_2$ values and higher wind speeds in August 2016. In contrast, narrow and elongated fjords such as those present along the east coast of Greenland (Kong Oscar Fjord and Kejser Franz Joseph Fjord) exhibited lower CO_2 uptake, a product of both smaller $\Delta p\text{CO}_2$ but also more calm summer wind conditions.

In fact, large uncertainty remains in estimating flux magnitudes based upon the source of wind data as well as the choice of gas transfer velocity parameterization. For instance, Sejr et al. (2011) reported larger flux magnitudes in Young Sound, registering below $-25 \text{ mmol m}^{-2} \text{ day}^{-1}$, compared to our range of -4 to $-10 \text{ mmol m}^{-2} \text{ day}^{-1}$ despite relatively similar $\Delta p\text{CO}_2$ measurements between 2006-2009 and during this study conducted in 2018. The discrepancies in flux calculations primarily stem from differences in wind speed measurements. Sejr et al. (2011) relied on hourly wind speeds from a nearby weather station, recording higher wind speeds compared to estimates derived from the Copernicus Arctic Reanalysis (2021). The non-linear relationship with wind speed results in intermittent spikes of gas transfer during periods of high wind speeds, enabling a large portion of monthly air-sea exchange to occur within a single storm.

The calculation of gas transfer velocities relies on empirically derived relationships. However, existing studies have primarily quantified k_{600} values in regions that are rather dissimilar to Arctic coastal ecosystems, making the choice of parameterization for coastal Greenland waters difficult. Even more worrying is the fact that the equation chosen to derive k_{600} significantly influences the magnitude of the fluxes we calculate (Fig. 5a). Currently, it remains unclear whether k_{600} values derived from open-ocean, coastal, or estuarine systems best represent Arctic fjords. In our study, this choice results in substantial variations, changing the maximum measured air-sea exchange from -24.8 to $-61.6 \text{ mmol m}^{-2} \text{ day}^{-1}$ and altering median values from -2.5 to $-15.9 \text{ mmol m}^{-2} \text{ day}^{-1}$. Comparing Greenland coastal fluxes using Borges et al. (2014) and Wanninkhof & McGillis (1999) parameterizations results in an average flux difference of 772%. Uncertainties based on gas parameterization increase with both faster wind speeds and larger air-sea differences in $p\text{CO}_2$ (Fig. 5b). While Greenland fjords may not exhibit high wind speeds in the summer season, they certainly demonstrate extreme negative $\Delta p\text{CO}_2$ values, making this choice of gas transfer equation disproportionately important compared to ecosystems at lower latitudes. These considerable discrepancies underscore the pressing need for better establishment of transfer velocities specific to these coastal Arctic regions.

Despite the uncertainties, we wanted to place this study in context by comparing to other coastal estimates of CO_2 sequestration. Upscaling of coastal carbon fluxes, particularly at high latitudes, is often based upon few datapoints/study sites (Laruelle et al., 2013). This study demonstrates the large heterogeneity of Greenland's coastlines and oceanographic conditions, therefore putting to question the reliability of upscaling efforts based on data from few locations. To compare with these assessments, we estimate coastal Greenland uptake by multiplying mean flux rates for fjord and shelf waters with estuarine and shelf surface areas according to Laruelle et al. (2013), obtaining uptake rates of $0.056 \pm 0.052 \text{ Tg C day}^{-1}$. An annual estimate of Greenland coastal uptake was then calculated based upon these August flux rates and then scaled by the yearly-averaged ice cover in the estuarine and shelf regional areas according to Laruelle et al (2014), assuming no gas transfer

447 where sea ice was present (Sejr et al., 2011). Assuming North and South Greenland coasts have
448 63.5% and 25.4% yearly-averaged ice cover respectively, we obtain the total Greenland coastal
449 uptake rates of $-9.5 \pm 9.0 \text{ Tg C year}^{-1}$. We recognize this annual estimate makes many assumptions,
450 especially as previous studies indicate large seasonality in carbon dynamics and air-sea exchange in
451 Greenland fjords (Meire et al., 2023, 2015; Rysgaard et al., 2012). However, for the sake of
452 comparison and context we present this first order estimate. Both Laruelle et al. (2014) and Dai et
453 al. (2022) report nearly two to three times higher carbon sequestration in this region (-16.37 and $-$
454 $26.44 \text{ Tg C year}^{-1}$ respectively). Indeed, this region is beset by wide ranging estimates of air-sea
455 exchange, partly due to the choice of gas-transfer parameterization. Still, based upon this study's,
456 perhaps conservative, CO_2 uptake rates, the Greenland coastal ocean represents 3.8% of global
457 coastal CO_2 uptake ($0.25 \text{ Pg C year}^{-1}$) and 7.1% of uptake in the Arctic coastal zone ($-134 \text{ Tg C year}^{-1}$;
458 Dai et al., 2022) despite constituting 2.9% of global coastal ocean area (Laruelle et al., 2013). This
459 considerable percentage of global carbon storage in such a relatively small region reiterates the
460 need to better resolve this highly variable region with regards to carbon dynamics and air-sea
461 exchange.
462

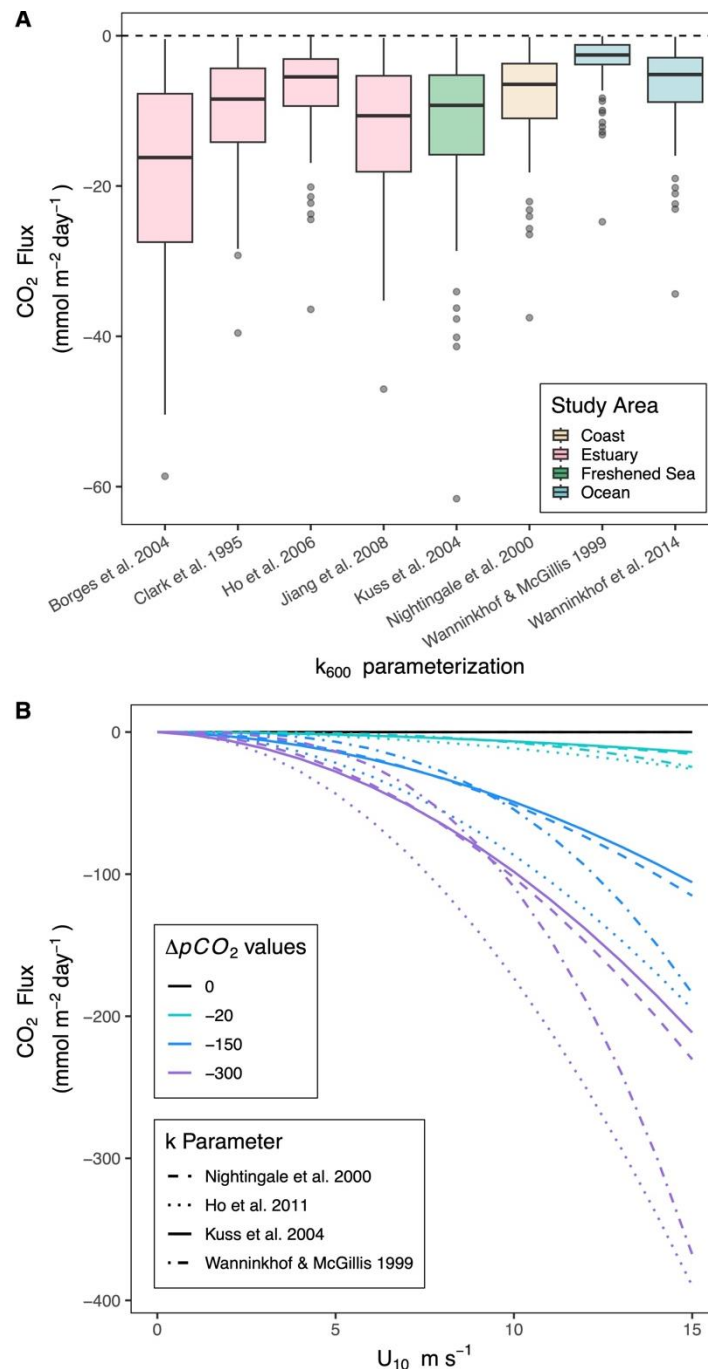


Figure 5. Calculated flux from coastal Greenland waters using different gas transfer velocity parameterizations (Borges et al., 2004; Wanninkhof and McGillis, 1999; Nightingale et al., 2000; Jiang et al., 2015; Kuss et al., 2004; Ho et al., 2011; Wanninkhof, 2014; Clark et al., 1995) (a). Variability in CO₂ uptake explained by wind speed, ΔpCO₂ magnitude, and choice of gas parameterization.

Conclusion

The widespread undersaturation of surface water pCO₂ in Greenlandic coastal waters confirms that this region acts as a carbon sink during summer. However, pCO₂ concentrations as well as air-sea exchange rates exhibited considerable geographical variability. Levels of pCO₂ on the West coast of Greenland were controlled by a combination of biological and physical/chemical drivers. Levels of

net autotrophy/heterotrophy, indicated by oxygen saturation, combined with freshwater runoff helped to explain spatial variation in West coast pCO₂ levels. In contrast, East Greenland fjords had pCO₂ levels that were dictated mainly by abiotic factors, including temperature and salinity. Freshwater export has two-fold effects, altering primary production by modifying circulation in the surface layer and exerting direct physical/chemical impacts. Therefore, the lowest pCO₂ values and the largest air-sea exchange occurred on the West coast of Greenland where high levels of net production and freshwater export took place concurrently. This resulted in CO₂ uptake reaching -38 mmol m⁻² day⁻¹. Using these measurements across 6° of latitude, allowed us to create a first order estimate of CO₂ uptake in the Greenland coastal ocean. Using average fluxes in fjords and shelf waters combined with coastal surface area data indicated that the Greenland coastal ocean absorbs -9.5 ± 9.0 Tg C year⁻¹, or nearly 4% of global coastal ocean CO₂ uptake. However, quantifying the *true* flux magnitude is beset by significant uncertainties (up to 770%), stemming from the averaging of wind products, as well as the selection of gas exchange formulations. We therefore encourage further studies to refine the estimation of gas transfer velocities in the Arctic coastal zone, as this represents the largest contributor to present uncertainty. Additionally, comprehensive understanding demands data collection across multiple seasons. This expanded temporal scope will provide a more holistic view of the year-round dynamics of CO₂ exchange within Greenlandic fjords, shedding light on how these ecosystems sequester carbon throughout the annual cycle.

Acknowledgements

We thank the captains and crews of RV Sanna and HDMS Lauge Koch, as well as Eik Britsch and Egon Frandsen for logistical support. This study is a contribution to the GreenFeedback project (Greenhouse gas fluxes and earth system feedbacks, grant agreement: 101056921), funded by the European Union under the Horizon Europe program. Cruises were funded by Danish Centre for Marine Science (Grants: 2016-05 and 2017-06). H.C.H. was supported by the AUFF (Aarhus Universitets Forskningsfond, project no. AUFF-F-2021 -7-7) as part of his PhD. J.M.H. was supported by Horizon 2020 FACE-IT project, under grant agreement no. 869154, and the Danmarks Frie Forskningsfond, project number 1131-00019B. L.M. was funded by research programme VENI with project number 016.Veni.192.150, which is financed by the Dutch Research Council (NWO). M.S. was funded by the project Polar Ocean Mitigation Potential (European commission grant no. 101136875). Data from the Greenland Ecosystem Monitoring Programme were provided by the Greenland Institute of Natural Resources, Nuuk, Greenland in collaboration with Department of Ecoscience, Aarhus University, Denmark. Views and opinions expressed in this publication are those of the authors only and do not necessarily reflect those of the European Union. The European Union cannot be held responsible for them.

Data Availability

Data relevant to reproduce the results of this study have been made available on Zenodo, an all-purpose open research repository created by Open Access Infrastructure for Research in Europe (OPENAire), a project supported by the European Commission, and by CERN, the European Organization for Nuclear Research. Oceanic pCO₂ data are available with the following DOI: <https://doi.org/10.5281/zenodo.10679593>. Environmental variables recorded by CTD instruments are available for cruises from the West and East coasts respectively at the following DOIs: <https://doi.org/10.5281/zenodo.4062024> and <https://doi.org/10.5281/zenodo.5572329>.

CRedit authorship contribution statement

Henry Henson: Conceptualization, Formal analysis, Data curation, Writing – original draft. Mikael Sejr: Investigation, Writing – review & editing. Lorenz Meire: Investigation, Writing – review & editing. Mie Winding: Investigation, Writing – review& editing. Lise Lotte Sørensen: Supervision,

Funding acquisition, Writing – review & editing. Johnna M. Holding: Conceptualization, Investigation, Supervision, Funding acquisition, Writing – review & editing.

Declaration of competing interest

The authors declare that they have no known competing financial interests or personal relationships that could have appeared to influence the work reported in this paper.

References

- Ahmed, M. M. M., Else, B. G. T., Capelle, D., Miller, L. A., and Papakyriakou, T.: Underestimation of surface p CO₂ and air-sea CO₂ fluxes due to freshwater stratification in an Arctic shelf sea, Hudson Bay, *Elementa: Science of the Anthropocene*, 8, 084, <https://doi.org/10.1525/elementa.084>, 2020.
- Anderson, L. G., Jutterström, S., Hjalmarsson, S., Wåhlström, I., and Semiletov, I. P.: Outgassing of CO₂ from Siberian Shelf seas by terrestrial organic matter decomposition, *Geophysical Research Letters*, 36, <https://doi.org/10.1029/2009GL040046>, 2009.
- Arendt, K. E., Nielsen, T., Rysgaard, S., and Tønnesson, K.: Differences in plankton community structure along the Godthåbsfjord, from the Greenland Ice Sheet to offshore waters, *Mar. Ecol. Prog. Ser.*, 401, 49–62, <https://doi.org/10.3354/meps08368>, 2010.
- Azetsu-Scott, K., Clarke, A., Falkner, K., Hamilton, J., Jones, E. P., Lee, C., Petrie, B., Prinsenber, S., Starr, M., and Yeats, P.: Calcium carbonate saturation states in the waters of the Canadian Arctic Archipelago and the Labrador Sea, *J. Geophys. Res.*, 115, C11021, <https://doi.org/10.1029/2009JC005917>, 2010.
- Bates, N. R. and Mathis, J. T.: The Arctic Ocean marine carbon cycle: evaluation of air-sea CO₂ exchanges, ocean acidification impacts and potential feedbacks, 2009.

571 Bendtsen, J., Mortensen, J., Lennert, K., K. Ehn, J., Boone, W., Galindo, V., Hu, Y.,
572 Dmitrenko, I. A., Kirillov, S. A., Kjeldsen, K. K., Kristoffersen, Y., G. Barber, D., and
573 Rysgaard, S.: Sea ice breakup and marine melt of a retreating tidewater outlet glacier in
574 northeast Greenland (81°N), *Sci Rep*, 7, 4941, <https://doi.org/10.1038/s41598-017-05089-3>,
575 2017.

576 Borges, A. V., Vanderborght, J.-P., Schiettecatte, L.-S., Gazeau, F., Ferrón-Smith, S.,
577 Delille, B., and Frankignoulle, M.: Variability of the gas transfer velocity of CO₂ in a
578 macrotidal estuary (the Scheldt), *Estuaries*, 27, 593–603,
579 <https://doi.org/10.1007/BF02907647>, 2004.

580 Carlson, D. F., Holding, J. M., Bendtsen, J., Markager, S., Møller, E. F., Meire, L., Rysgaard,
581 S., Dalsgaard, T., and Sej, M. K.: CTD Profiles from the R/V Sanna cruise to Northwest
582 Greenland fjords, August 11–31, 2016, <https://doi.org/10.5281/zenodo.4062024>, 2020.

583 Chen, C.-T. A. and Borges, A. V.: Reconciling opposing views on carbon cycling in the
584 coastal ocean: Continental shelves as sinks and near-shore ecosystems as sources of
585 atmospheric CO₂, *Deep Sea Research Part II: Topical Studies in Oceanography*, 56, 578–
586 590, <https://doi.org/10.1016/j.dsr2.2009.01.001>, 2009.

587 Chierici, M. and Fransson, A.: Calcium carbonate saturation in the surface water of the
588 Arctic Ocean: undersaturation in freshwater influenced shelves, *Biogeosciences*, 6, 2421–
589 2432, <https://doi.org/10.5194/bg-6-2421-2009>, 2009.

590 Christensen, T. R., Topp-Jørgensen, E., Sej, M. K., and Schmidt, N. M.: Foreword:
591 Synthesis of the Greenland Ecosystem Monitoring program, *Ambio*, 46, 1–2,
592 <https://doi.org/10.1007/s13280-016-0860-z>, 2017.

593 Ciais, P., Gasser, T., Paris, J. D., Caldeira, K., Raupach, M. R., Canadell, J. G., Patwardhan,
594 A., Friedlingstein, P., Piao, S. L., and Gitz, V.: Attributing the increase in atmospheric CO₂
595 to emitters and absorbers, *Nature Clim Change*, 3, 926–930,
596 <https://doi.org/10.1038/nclimate1942>, 2013.

597 Clark, J. F., Schlosser, P., Simpson, H. J., Stute, M., Wanninkhof, R., and Ho, D. T.:
598 Relationship between gas transfer velocities and wind speeds in the tidal Hudson River
599 determined by the dual tracer technique, *Air-water gas transfer*, 785–800, 1995.

600 Copernicus Climate Change Service: Arctic regional reanalysis on single levels from 1991 to
601 present, <https://doi.org/10.24381/CDS.713858F6>, 2021.

602 Dai, M., Su, J., Zhao, Y., Hofmann, E. E., Cao, Z., Cai, W.-J., Gan, J., Lacroix, F., Laruelle, G.
603 G., Meng, F., Müller, J. D., Regnier, P. A. G., Wang, G., and Wang, Z.: Carbon Fluxes in the
604 Coastal Ocean: Synthesis, Boundary Processes, and Future Trends, *Annu. Rev. Earth*
605 *Planet. Sci.*, 50, 593–626, <https://doi.org/10.1146/annurev-earth-032320-090746>, 2022.

606 Ericson, Y., Falck, E., Chierici, M., Fransson, A., and Kristiansen, S.: Marine CO₂ system
607 variability in a high arctic tidewater-glacier fjord system, Tempelfjorden, Svalbard,
608 *Continental Shelf Research*, 181, 1–13, <https://doi.org/10.1016/j.csr.2019.04.013>, 2019.

609 Fay, A. R., Gregor, L., Landschützer, P., McKinley, G. A., Gruber, N., Gehlen, M., Iida, Y.,
610 Laruelle, G. G., Rödenbeck, C., Roobaert, A., and Zeng, J.: SeaFlux: harmonization of air–
611 sea CO₂ fluxes from surface pCO₂ data products using a standardized approach, *Earth*
612 *System Science Data*, 13, 4693–4710, <https://doi.org/10.5194/essd-13-4693-2021>, 2021.

613 Fietzek, P., Fiedler, B., Steinhoff, T., and Körtzinger, A.: In situ Quality Assessment of a
614 Novel Underwater pCO₂ Sensor Based on Membrane Equilibration and NDIR
615 Spectrometry, *Journal of Atmospheric and Oceanic Technology*, 31, 181–196,
616 <https://doi.org/10.1175/JTECH-D-13-00083.1>, 2014.

617 Fransson, A., Chierici, M., Nomura, D., Granskog, M. A., Kristiansen, S., Martma, T., and
618 Nehrke, G.: Effect of glacial drainage water on the CO₂ system and ocean acidification
619 state in an Arctic tidewater-glacier fjord during two contrasting years, *J. Geophys. Res.*
620 *Oceans*, 120, 2413–2429, <https://doi.org/10.1002/2014jc010320>, 2015.

621 Granskog, M. A., Kuzyk, Z. Z. A., Azetsu-Scott, K., and Macdonald, R. W.: Distributions of
622 runoff, sea-ice melt and brine using δ¹⁸O and salinity data — A new view on freshwater
623 cycling in Hudson Bay, *Journal of Marine Systems*, 88, 362–374,
624 <https://doi.org/10.1016/j.jmarsys.2011.03.011>, 2011.

625 Gregor, L.: SeaFlux v2023: harmonised sea-air CO₂ fluxes from surface pCO₂ data products
626 using a standardised approach, <https://doi.org/10.5281/zenodo.8280457>, 2023.

627 Henley, S. F., Porter, M., Hobbs, L., Braun, J., Guillaume-Castel, R., Venables, E. J.,
628 Dumont, E., and Cottier, F.: Nitrate supply and uptake in the Atlantic Arctic sea ice zone:
629 seasonal cycle, mechanisms and drivers, *Philosophical Transactions of the Royal Society A:*
630 *Mathematical, Physical and Engineering Sciences*, 378, 20190361,
631 <https://doi.org/10.1098/rsta.2019.0361>, 2020.

632 Henson, H. C., Holding, J. M., Meire, L., Rysgaard, S., Stedmon, C. A., Stuart-Lee, A.,
633 Bendtsen, J., and Sejr, M.: Coastal freshening drives acidification state in Greenland fjords,
634 *Science of The Total Environment*, 855, 158962,
635 <https://doi.org/10.1016/j.scitotenv.2022.158962>, 2023.

636 Ho, D. T., Schlosser, P., and Orton, P. M.: On Factors Controlling Air–Water Gas Exchange
637 in a Large Tidal River, *Estuaries and Coasts*, 34, 1103–1116, [https://doi.org/10.1007/s12237-](https://doi.org/10.1007/s12237-011-9396-4)
638 [011-9396-4](https://doi.org/10.1007/s12237-011-9396-4), 2011.

639 Holding, J. M., Carlson, D. F., Meire, L., Stuart-Lee, A., Møller, E. F., Markager, S., Lund-
640 Hansen, L., Stedmon, C., Britsch, E., and Sejr, M. K.: CTD Profiles from the HDMS Lauge
641 Koch cruise to East Greenland fjords, August 2018, <https://doi.org/10.5281/zenodo.5572329>,
642 2021.

643 Jiang, L.-Q., Feely, R. A., Carter, B. R., Greeley, D. J., Gledhill, D. K., and Arzayus, K. M.:
644 Climatological distribution of aragonite saturation state in the global oceans: ARAGONITE
645 SATURATION CLIMATOLOGY, *Global Biogeochem. Cycles*, 29, 1656–1673,
646 <https://doi.org/10.1002/2015GB005198>, 2015.

647 Kreft, H. and Jetz, W.: Global patterns and determinants of vascular plant diversity,
648 Proceedings of the National Academy of Sciences, 104, 5925–5930,
649 <https://doi.org/10.1073/pnas.0608361104>, 2007.

650 Kuss, J., Nagel, K., and Schneider, B.: Evidence from the Baltic Sea for an enhanced CO₂
651 air—sea transfer velocity, Tellus B: Chemical and Physical Meteorology, 56, 175–182,
652 <https://doi.org/10.3402/tellusb.v56i2.16407>, 2004.

653 Laruelle, G. G., Dürr, H. H., Lauerwald, R., Hartmann, J., Slomp, C. P., Goossens, N., and
654 Regnier, P. a. G.: Global multi-scale segmentation of continental and coastal waters from
655 the watersheds to the continental margins, Hydrology and Earth System Sciences, 17,
656 2029–2051, <https://doi.org/10.5194/hess-17-2029-2013>, 2013.

657 Laruelle, G. G., Lauerwald, R., Pfeil, B., and Regnier, P.: Regionalized global budget of the
658 CO₂ exchange at the air-water interface in continental shelf seas, Global Biogeochemical
659 Cycles, 28, 1199–1214, <https://doi.org/10.1002/2014GB004832>, 2014.

660 Laruelle, G. G., Cai, W.-J., Hu, X., Gruber, N., Mackenzie, F. T., and Regnier, P.: Continental
661 shelves as a variable but increasing global sink for atmospheric carbon dioxide, Nat
662 Commun, 9, 454, <https://doi.org/10.1038/s41467-017-02738-z>, 2018.

663 Macovei, V. A., Voynova, Y. G., Becker, M., Triest, J., and Petersen, W.: Long-term
664 intercomparison of two *P* CO₂ instruments based on ship-of-opportunity measurements in
665 a dynamic shelf sea environment, Limnology & Ocean Methods, 19, 37–50,
666 <https://doi.org/10.1002/lom3.10403>, 2021.

667 Meire, L., Søgaard, D. H., Mortensen, J., Meysman, F. J. R., Soetaert, K., Arendt, K. E., Juul-
668 Pedersen, T., Blicher, M. E., and Rysgaard, S.: Glacial meltwater and primary production are
669 drivers of strong CO₂ uptake in fjord and coastal waters adjacent to the Greenland Ice
670 Sheet, Biogeosciences, 12, 2347–2363, <https://doi.org/10.5194/bg-12-2347-2015>, 2015.

671 Meire, L., Mortensen, J., Meire, P., Juul-Pedersen, T., Sejr, M. K., Rysgaard, S., Nygaard, R.,
672 Huybrechts, P., and Meysman, F. J. R.: Marine-terminating glaciers sustain high
673 productivity in Greenland fjords, Glob Change Biol, 23, 5344–5357,
674 <https://doi.org/10.1111/gcb.13801>, 2017.

675 Meire, L., Paulsen, M. L., Meire, P., Rysgaard, S., Hopwood, M. J., Sejr, M. K., Stuart-Lee,
676 A., Sabbe, K., Stock, W., and Mortensen, J.: Glacier retreat alters downstream fjord
677 ecosystem structure and function in Greenland, Nat. Geosci., 16, 671–674,
678 <https://doi.org/10.1038/s41561-023-01218-y>, 2023.

679 Miller, L. A., Burgers, T. M., Burt, W. J., Granskog, M. A., and Papakyriakou, T. N.: Air-Sea
680 CO₂ Flux Estimates in Stratified Arctic Coastal Waters: How Wrong Can We Be?, Geophys.
681 Res. Lett., 46, 235–243, <https://doi.org/10.1029/2018GL080099>, 2019.

682 Mortensen, J., Bendtsen, J., Lennert, K., and Rysgaard, S.: Seasonal variability of the
683 circulation system in a west Greenland tidewater outlet glacier fjord, Godthåbsfjord (64°N):
684 Godthåbsfjord, J. Geophys. Res. Earth Surf., 119, 2591–2603,
685 <https://doi.org/10.1002/2014JF003267>, 2014.

686 Nightingale, P. D., Malin, G., Law, C. S., Watson, A. J., Liss, P. S., Liddicoat, M. I., Boutin, J.,
687 and Upstill-Goddard, R. C.: In situ evaluation of air-sea gas exchange parameterizations
688 using novel conservative and volatile tracers, *Global Biogeochemical Cycles*, 14, 373–387,
689 <https://doi.org/10.1029/1999GB900091>, 2000.

690 Rysgaard, S., Mortensen, J., Juul-Pedersen, T., Sørensen, L. L., Lennert, K., Søgaard, D. H.,
691 Arendt, K. E., Blicher, M. E., Sejr, M. K., and Bendtsen, J.: High air–sea CO₂ uptake rates in
692 nearshore and shelf areas of Southern Greenland: Temporal and spatial variability, *Marine*
693 *Chemistry*, 128–129, 26–33, <https://doi.org/10.1016/j.marchem.2011.11.002>, 2012.

694 Sabine, C. L.: The Oceanic Sink for Anthropogenic CO₂, *Science*, 305, 367–371,
695 <https://doi.org/10.1126/science.1097403>, 2004.

696 Sejr, M. K., Krause-Jensen, D., Rysgaard, S., Sørensen, L. L., Christensen, P. B., and Glud, R.
697 N.: Air–sea flux of CO₂ in arctic coastal waters influenced by glacial melt water and sea ice,
698 *Tellus B: Chemical and Physical Meteorology*, 63, 815–822, [https://doi.org/10.1111/j.1600-](https://doi.org/10.1111/j.1600-0889.2011.00540.X)
699 [0889.2011.00540.X](https://doi.org/10.1111/j.1600-0889.2011.00540.X), 2011.

700 Sejr, M. K., Krause-Jensen, D., Dalsgaard, T., Ruiz-Halpern, S., Duarte, C. M., Middelboe,
701 M., Glud, R. N., Bendtsen, J., Balsby, T. J. S., and Rysgaard, S.: Seasonal dynamics of
702 autotrophic and heterotrophic plankton metabolism and PCO₂ in a subarctic Greenland
703 fjord, *Limnol. Oceanogr.*, 59, 1764–1778, <https://doi.org/10.4319/l0.2014.59.5.1764>, 2014.

704 Takahashi, T., Sutherland, S. C., Wanninkhof, R., Sweeney, C., Feely, R. A., Chipman, D. W.,
705 Hales, B., Friederich, G., Chavez, F., Sabine, C., Watson, A., Bakker, D. C. E., Schuster, U.,
706 Metzl, N., Yoshikawa-Inoue, H., Ishii, M., Midorikawa, T., Nojiri, Y., Körtzinger, A.,
707 Steinhoff, T., Hoppema, M., Olafsson, J., Arnarson, T. S., Tilbrook, B., Johannessen, T.,
708 Olsen, A., Bellerby, R., Wong, C. S., Delille, B., Bates, N. R., and de Baar, H. J. W.:
709 Climatological mean and decadal change in surface ocean pCO₂, and net sea–air CO₂ flux
710 over the global oceans, *Deep Sea Research Part II: Topical Studies in Oceanography*, 56,
711 554–577, <https://doi.org/10.1016/j.dsr2.2008.12.009>, 2009.

712 Velicogna, I., Mohajerani, Y., A. G., Landerer, F., Mouginit, J., Noel, B., Rignot, E.,
713 Sutterley, T., van den Broeke, M., van Wessem, M., and Wiese, D.: Continuity of Ice Sheet
714 Mass Loss in Greenland and Antarctica From the GRACE and GRACE Follow-On Missions,
715 *Geophysical Research Letters*, 47, e2020GL087291, <https://doi.org/10.1029/2020GL087291>,
716 2020.

717 Vernet, M., Ellingsen, I., Marchese, C., Bélanger, S., Cape, M., Slagstad, D., and Matrai, P.
718 A.: Spatial variability in rates of net primary production (NPP) and onset of the spring
719 bloom in Greenland shelf waters, *Progress in Oceanography*, 198,
720 <https://doi.org/10.1016/j.pocean.2021.102655>, 2021.

721 Wanninkhof, R.: Relationship between wind speed and gas exchange over the ocean
722 revisited, *Limnology and Oceanography: Methods*, 12, 351–362,
723 <https://doi.org/10.4319/lom.2014.12.351>, 2014.

724 Wanninkhof, R. and McGillis, W. R.: A cubic relationship between air-sea CO₂ exchange and
725 wind speed, *Geophysical Research Letters*, 26, 1889–1892,
726 <https://doi.org/10.1029/1999GL900363>, 1999.

727